Interesterification of triglycerides with methyl acetate for biodiesel production using a cyclodextrin-derived SnO@γ-Al₂O₃ composite as heterogeneous catalyst

Claudia Prestigiacomo[a], Martina Biondo[a,b], Alessandro Galia[a,*], Eric Monflier[b], Anne Ponchel[b], Dominique Prevost[b], Onofrio Scialdone[a], Sebastien Tilloy[b], Rudina Bleta[b,*]

[a]Dipartimento di Ingegneria, Sezione Chimica Ambientale Biomedica Idraulica e dei Materiali, Università degli Studi di Palermo, Viale delle Scienze, 90128 Palermo, Italy

[b]Univ. Artois, CNRS, Centrale Lille, Univ. Lille, UMR 8181-UCCS-Unité de Catalyse et Chimie du Solide, F-62300 Lens, France.

*Corresponding authors: Alessandro Galia, Rudina Bleta
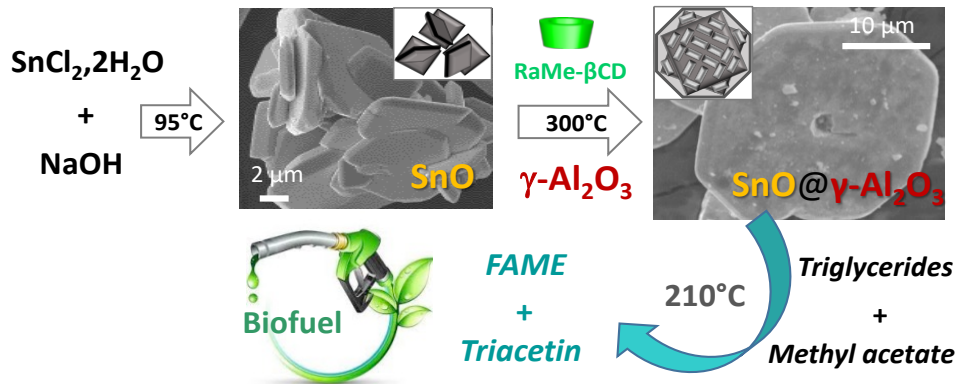**alessandro.galia@unipa.it**
rudina.bleta@univ-artois.fr

Graphical abstract

SnCl₂,2H₂O + NaOH — 95°C → SnO — RaMe-βCD, 300°C, γ-Al₂O₃ → SnO@γ-Al₂O₃ — 210°C → Triglycerides + Methyl acetate → FAME + Triacetin → Biofuel

1

2   **Abstract**

3   Particle morphology and surface properties of metal oxides are topics of great importance in the field

4   of heterogeneous catalysis. Herein, we have developed a molecular-colloidal coassembly approach

5   combined with an ultrasonic-assisted precipitation method to fabricate $SnO@\gamma-Al_2O_3$ composites

6   with tuneable pore size and well-defined octahedral-shape crystal structure. The supramolecular

7   assemblies formed between the randomly methylated β-cyclodextrin (RaMeβCD) and Pluronic F127

8   were employed as template to tailor the size and shape of $\gamma-Al_2O_3$ nanoparticles and direct their

9   assembly almost exclusively on the surface of micrometer-sized SnO single crystals. Results revealed

10   that the cooperative action of the supramolecular template and $\gamma-Al_2O_3$ nanoparticles may have a

11   critical effect on the growth and orientation of SnO microcrystals and ultimately determine their

12   catalytic performance in the interesterification of rapeseed oil with methyl acetate. The

13   compartmentalized $SnO@\gamma-Al_2O_3$ structures could achieve a fatty acid methyl esters (FAME) yield

14   of 33.5% after 30 min and 82.5 % after 120 minutes at 210 °C, exceeding by 42% that of the

15   commercial catalyst.

16

17   **1. Introduction**

18   The current energy system for transportation is still based on fossil fuels whose utilization is not

19   sustainable in the long term due to limited resources and negative impact on climate change related

20   to the accumulation of CO_2 in the atmosphere [1]. For these reasons, fossil fuels must be gradually

21   substituted by other CO_2 neutral renewable energetic sources. In this context, biodiesel can be an

22   interesting renewable alternative to fossil diesel as it has similar performances, but lower emissions

23   of particulate matter and greenhouse gases [2].

24   The conventional industrial route to biodiesel (fatty acid methyl esters or FAME) production is by

25   transesterification of triglycerides (TG) contained in fatty feedstocks, such as vegetable oils or animal

fats, with excess methanol [3] using acid or base chemical catalysts [4], as well as enzymes [5]. Although transesterification has been widely used for FAME production, this technology presents some drawbacks, such as the generation of glycerol as a byproduct, which is usually managed as a waste. In fact, thevast amount of crude glycerol generated each year largely exceeds the current demand for chemical production in the market and the disposal of waste glycerol has become a serious environmental issue that needs to be resolved within the next decade. Another drawback of the transesterification is that methanol, which is used as acyl acceptor, is insoluble in the reaction media; therefore the alcoholysis generally starts with high interfacial mass transfer resistances that require accurate mixing. Recently, it was also found that methanol could be incompatible with the long-term stability of several heterogeneous catalytic systems, therefore making the overall process less effective [1].

To overcome those limitations, other biodiesel production technologies have been developed so far [6,7]. In particular, the interesterification of triglycerides has been identified as a promising alternative to the transesterification route sincemethanol is substituted with methyl or ethyl acetate as acyl donors, which are perfectly miscible with the reactive mixture [8]. In addition, the triacetylglycerol (triacetin, TA) generated as the main co-product, has a higher market value compared to glycerol since it can be added to the biodiesel formulation up to 10 wt.%, without changing the fuel quality [9], and can also be usedas green plasticiser for polymers and as additive in cosmetic and pharmaceutical industries [10].

Many studies were conducted in the last years to investigate the potentiality of the interesterification in order to optimize the operative parameters and the performances of the catalytic system. Some of them evidence that this reaction could be performed without added catalysts,using supercritical methyl acetate [1,11-15] or ethyl acetate [16,17] as acyl donnors, but the high-temperature and high-pressure conditions reduce the process flexibility. Other studies report that the interesterification can be conducted at room temperature using alkaline hydroxide and/or alkoxides as homogeneous catalysts [18-25]. However, as alkaline compounds are only partially soluble in the reaction mixture,

low molecular weight poly(ethyleneglycol) is usually employed as complexing agent, or hazardous

solvents, such as tetrahydrofuran, are added to the reaction mixture to improve the reaction kinetics

[19,20]. In another study, tin (II) octoate was identified as an efficient homogeneous catalyst in the

interesterification of rapeseed oil with ethyl acetate acieving 61% fatty acid ethyl esters (FAEE) yield

after 20 h at 210 °C [26].Although tin (II) octoate was completely soluble in the reaction system, its

recovery was a serious drawback for the practical use of the process. In addition, enzymes have also

been extensively employed as biocatalysts in the interesterification of vegetable oils with different

acyl donors [27-32]. Enzymes offer the advantage of conducting the reaction under mild conditions,

giving near quantitative FAME yields with almost no activity loss upon reuse, but they fail to achieve

high yields in short reaction times [32,33].

In this context, chemical heterogeneous interesterification has aroused as an interesting alternative

since it offers the advantage of producing high FAME yields in short reaction times and the possibility

to regenerate and reuse the catalyst, therefore reducing the operation costs. From the literature on this

field, it seems however that interesterification usually requires longer reaction times with respect to

transesterification to reach equivalent FAME yields [1]. Phenyl-sulfonic acid-functionalized SBA-15

catalyst [34],nobium phosphate, nobium oxide, γ-alumina and zeolite HY [35,36], together with

mixed oxides [37] and hydrotalcites [38], were investigated as heterogeneous catalysts in the

interesterification of several raw materials at different operational conditions. In particular, 48%

FAME yield was obtained in the interesterification of olive oil with ethyl acetate after 6 h at 130 °C

in the presence of phenyl-sulfonic acid-functionalized SBA-15 [34], while 52.5% and 49.8 % FAME

yields could be reached in the interesterification of macaw oil with methyl acetate after 1 h at 250°C

using γ-alumina and nobium phosphate, respectively, as heterogeneous catalysts [35].

Recently, commercial Sn(II)O has been identified as a promising heterogeneous catalyst in the

interesterification of rapeseed oil with methyl acetate [39]. Unfortunately, this material was composed

of agglomerated particles with extremely low surface area ($0.7 \ m^2/g$) and pore volume ($0.0022 \ cm^3/g$)

which may cause inevitable mass transfer limitations during the catalytic process, leading to a

decrease of the catalyst utilization efficiency. Therefore, finding a way to control the morphology and surface properties of Sn(II)O and at the same time increase the availability of catalytic active sites is of significant importance for optimizing the catalyst performance.

In this context, the application of γ-alumina (γ-Al$_2$O$_3$) as support material is an attractive option for increasing metal-support interactions owing to the great number of γ-Al$_2$O$_3$ surface defects that are known to play an important role as binding sites for catalytic particles and clusters [40,41]. In a previous study [42], we have proposed for the first time an efficient cyclodextrin (CD)-assisted colloidal self-assembly strategy to synthesize γ-Al$_2$O$_3$-supported CoMo catalysts with excellent catalytic activity and stability in the hydrothermal liquefaction (HTL) of microalgae. In particular, randomly methylated β-cyclodextrin (RaMeβCD) with an average degree of methylation of 1.8 methoxy groups per glycopyranose unit and surface active properties [43] was found to be particularly effective in directing the assembly of AlO(OH) colloids around the metallo-supramolecular assemblies, giving rise to robust and reutilisable composites with high energy recovery capacity and promising oxygen removal efficiency.

Herein, we explore the capacity of γ-Al$_2$O$_3$ nanoparticles to adsorb preferentially on the (001) facets of square-like SnO crystals and trigger their stacking into octahedron-like particles with well-defined mesoporous core-shell micro-/nano-structure. The resulting composites demonstrate a remarkable improvement in the efficiency of interesterification of rapeseed oil with methyl acetate at 210°C with respect to commercial SnO, showing an increase by 42% in FAME yield. This study highlights a novel function of γ-Al$_2$O$_3$ to act not only as support material for dispersion of active elements, but also to modulate the shape of micron-sized SnO crystals and construct composites with new architectures and improved catalytic activity.

2. Materials and Methods

2.1 Materials

Tin (II) chloride dehydrate ($SnCl_2 \cdot 2H_2O$, Mw 225.65 g mol^{-1}), aluminum tri-sec-butoxide ASB ($Al[OC(CH_3)_3]_3$, Mw 246.32 g mol^{-1})and Pluronic F127 ($PEO_{106}PPO_{70}PEO_{106}$: PEO = poly(ethylene oxide) and PPO = poly(propylene oxide)) (Mw 12600 g mol^{-1}) were purchased from Sigma Aldrich. Randomly methylated β-cyclodextrin (denoted RaMeβCD, average degree of molar substitution (DS) 1.8, Mw 1310 g mol^{-1}) was a gift from Wacker Chemie GmbH. Refined rapeseed oil was purchased from a local supermarket and its fatty acid composition was determined by quantitative transesterification as reported byKoohi Kamali *et al.*[44], using sodium methoxide (98%) from Alfa Aesar as homogeneous catalyst, methanol (HPLC grade 99.8%) from Sigma Aldrich as alcohol and citric acid (99%) from Sigma Aldrich as neutralizing agent. Methyl acetate (HPLC grade > 99.8%) from Carlo Erba Reagents was used as acyl donor in the interesterification reaction and as solvent to prepare samples for GC analyses. For the GC calibration, methyl palmitate (C 16:0, ≥99%), methyl stearate (C 18:0, ~99%), methyl oleate (C 18:1, ≥99%), methyl linoleate (C 18:2, ≥99%), triacetin (≥99%) and methyl heptadecanoate (≥99%) were purchased from Sigma Aldrich.

2.2 Determination of the composition of rapeseed oil

Fatty acid composition of adopted rapeseed oil is reported in Table 1. It was determined by quantitative conversion of an oil sample to FAMEs by transesterification with methanol in the presence of sodium methoxide that is the most active homogeneous catalyst for this reaction [44]. Loading procedure and product separation were performed according to procedure reported in the literature [44]. The reaction was carried out dissolving 200±5 mg of sodium methoxide in 20.00±0.01 g of methanol. This solution was mixed with 10.00±0.01 g of the rapeseed oil. To obtain quantitative conversion of all triglycerides, the alcohol was in strong stoichiometric excess compared to the oil. The reaction was performed at the normal boiling point of methanol with a reaction apparatus and experimental procedure described elsewhere [39].

Table 1. Fatty acid composition of the rapeseed oil used in this study.

Fatty acid	Symbol (C-length : no.=bonds)	% w/w
Palmitic acid	16:0	4.5
Stearic acid	18:0	1.5
Oleic acid	18:1	65.1
Linoleic acid	18:2	16.5
Linolenic acid	18:3	10.8

Transesterified rapeseed oil must contain also methyl esters of C 20:1 and C 22:1 fatty acids, howeverthese FAMEs could not be detected and quantified because of the lack of suitable pure standards. Anyway, their cumulative concentration in our rapeseed oil must be lower than 2% w/w as assessed by the summation of the mass fractions reported in Table 1, and FAME yields should be little affected by their presence.

2.3 Preparation of tin based oxides

Three different approaches were used for the preparation of tin-based oxides. In a first approach, called complexation [45], urea (1.5 g, 25 mmol) and NaOH (0.34 g, 8.5 mmol) were dissolved in 20 mL of distilled water, then added to 20 mL of an aqueous solution of tin (II) chloride $SnCl_2 \cdot 2H_2O$ (0.65 g, 2.9 mmol). The mixture was refluxed at 40 °C for 30 min, then put it in a refrigerator at 4°C overnight. The resulting precipitate was isolated by filtration, then washed several times with water and ethanol and finally calcined at 500 °C for 4 h. This sample was denoted Sn-CM. In a second procedure, named hydrothermal method [46], $SnCl_2 \cdot 2H_2O$ (1.128 g) was first dissolved in 10mL of absolute ethanol, then 30 mL of ammonia solution (25-28 wt%) was added. After homogenization, the mixture was sealed in a Teflon-lined stainless-steel autoclave at 130 °C for 15 hours. The solid precipitate was collected by centrifugation, washed several times with deionized water, then rinsed with ethanol and finally dried in an oven at 80°C overnight. This sample was denoted Sn-HT.In a

third approach named alkaline method [47],$SnCl_2 \cdot 2H_2O$ (0.5 g, 2.2 mmol) was dissolved in 20 mL of distilled water at 75 °C and maintained under stirring for 30 minutes. Afterwards, varying amounts of NaOH (1.0 to 2.0 g) were added and mixtures were heated at 95 °C under reflux for additional 3 hours. The obtained precipitates were collected by centrifugation, washed with deionized water and ethanol by several centrifugation/redispersion cycles, and finally calcined at 300 °C for 3 hours. Samples were identified according to the following notation: Sn-alk-x where x represents the NaOH concentration in the reaction medium varying from 0.25M to 0.75M.

2.4 Preparation of mesoporous γ-Al_2O_3

γ-Al_2O_3 was prepared using boehmite AlO(OH) as precursor was synthesized according to a previously reported sol-gel method [48]. Typically, 185 mL of hot distilled water (85 °C) was added rapidly to 25.3 g (0.1 mol) of ASB at a hydrolysis ratio (h = [H_2O]/[Al]) of 100. Afterwards, 0.47 mL of nitric acid ([HNO_3]/[Al] = 0.07) was added dropwise to peptise the hydroxide precipitate. The mixture was refluxed at 85 °C for 24h, then allowed to cool down naturally to room temperature. The resulting hydrosol was a stable transparent suspension of AlO(OH) nanoparticles (pH 4.5) having an aluminum concentration of 0.5 mol L^{-1}. Afterwards, Pluronic F127 (10 wt %) and RaMeβCD (50 mg mL^{-1}) were added successively to 150 mL of the above boehmite sol. After an equilibrium time of 24 h at room temperature, the hybrid sol was dried at 80 °C, then the recovered xerogel was calcined at 500 °C for 2 h giving a mesoporous γ-Al_2O_3 material.

2.5 Preparation of SnO-based composites

SnO-based composites were prepared by co-assembly of γ-Al_2O_3 nanoparticles with as-synthesized SnO microcrystals in an aqueous RaMeβCD solution. Typically, for an aluminum-tin equimolar composition, 1.5 g of as-synthesized SnO was dispersed in 40 mL of an aqueous solution of RaMeβCD (30 mg mL^{-1}), to which 565 mg of γ-Al_2O_3 was added. The suspension was exposed to

1   ultrasonic irradiation for 15 minutes (120W power, 80% amplitude, 3s pulse on, 1s pulse off), then

2   maintained under stirring at 75 °C until water was completely evaporated. Finally, the recovered solid

3   was calcined at 300 °C for 3 hours under air flow. Catalysts were denoted SnO@γ-Al$_2$O$_3$y where y

4   indicates the Al/Sn molar ratio varying from 0.5 to 2.0.

5

6   **2.6 Characterization methods**

7   *N$_2$-adsorption isotherms* were collected at -196 °C using an adsorption analyzer Micromeritics Tristar

8   3020. The specific surface areas were evaluated by the Brunauer-Emmet-Teller (BET) method [49]

9   and pore size distributions were determined using the Barrett-Joyner-Halenda (BJH) method

10 assuming a cylindrical pore structure [50].*Powder X-ray Diffraction (XRD)* patterns were recorded

11 using a Siemens D5000 X-ray diffractometer equipped with a Cu Kα radiation source in a Bragg-

12 Brentano configuration. XRD scans were run with a 2θ angle in the range of 10° < 2θ < 80° using a

13 0.02° step size and a counting time of 2 s per step. *Scanning electron microscopy (SEM)* observations

14 were recorded on a field emission gun scanning electron microscope (FE-SEM) (model Hitachi S-

15 4700) equipped with an Energy Dispersive X-ray (EDX) detector. An acceleration voltage of 5.0 kV

16 was used to minimize the accumulation of charges in the sample.

17

18 **2.7 Analytical methods**

19 The concentrations of methyl esters and triacetin in the samples were measured using a Agilent 7890B

20 Gas Chromatograph (GC) equipped with a RESTEK Superchrom FAMEWAX capillary column

21 (length 30 m, external diameter 0.32 mm,internal diameter 0.25 mm) and a Flame Ionization Detector

22 (FID). Helium 5.0 was used as carrier gas. The GC oven temperature was set at 165 °C for 22 min,

23 then it was increased with a heating rate of 5°Cmin^{-1} up to 220°C and maintained at that temperature

24 for 5 min. Calibration was accomplished for FAMEs and triacetin by preparing solutions of known

25 concentration of pure alkyl esters (C 16:0, C 18:0, C 18:1, C 18:2, C 18:3) and TA, using methyl

heptadecanoate as internal standards. Cumulative yields in fatty acid methyl esters Y_{FAME} and in triacetin Y_{TA} were computed according to equation 1:

$$Y_{FAME} = \frac{M_{FAME}}{M^0_{oil}} \qquad Y_{TA} = \frac{M_{TA}}{M^0_{oil}} \qquad (1)$$

where M_{FAME} and M_{TA} are the masses of free fatty acid methyl esters and triacetin determined through GC calibration and M^0_{oil} is the initial mass of rapeseed oil loaded in the reactor.

2.8 Experimental procedures for interesterification

Interesterification experiments were conducted in a stainless steel autoclave reactor with an internal volume of 20 mL. A needle valve was used to insulate the reactor during the reaction. In a typical experiment, 1.5±0.01 g of rapeseed oil and 5.1±0.01 g of methyl acetate were loaded in the reactor to obtain an oil/methyl acetate molar ratio of 1:40. The reactor was sealed and Argon was used to purge and pressurize it at a final pressure of about 2.5 bar. The reactor was heated with a heating rate of about 12°Cmin^{-1}by two heating cartridges inserted in an aluminum block. Reaction time was computed after the reaction temperature was reached. To stop the interesterification, the reactor was rapidly cooled to room temperature by immersion in an ice-water bath.

The system was opened and the products, including the catalyst, were recovered by adding about 3 g of methyl acetate. The monophasic solution was separated from the catalyst by centrifugation at 4000 rpm for 30 min. The liquid phase was recovered with a Pasteur pipette and stored in a glass vial. The catalyst was washed several times with methyl acetate to remove traces of wetting oil mixture, then dried in an oven at 60 °C overnight.
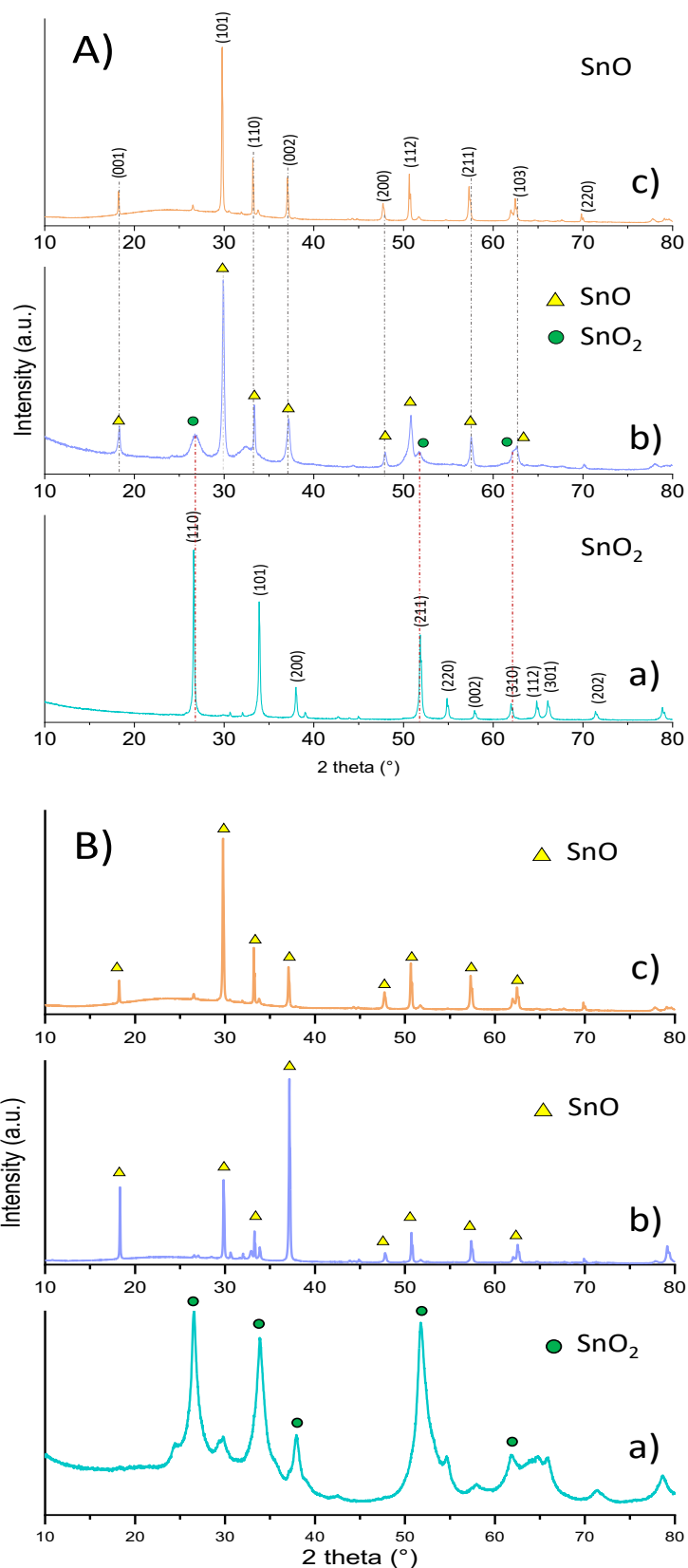
3. Results and discussion

3.1 Interesterification of rapeseed oil with bulk SnO catalysts

1 Initially, three different approaches were employed to prepare tin-based oxides with the goal to

2 evaluate the effect of the preparation method on the crystalline properties and interesterification

3 activity of the catalysts.

4 In a first approach, using urea as the complexing agent [45,51], cassiterite tetragonal Sn(IV)O$_2$

5 (JCPDS card 77-0450) was exclusively produced after calcination at 500 °C (Figure 1, Aa). On the

6 other hand, the hydrothermal synthesis carried out at 130°C for 16 hours [46] yielded a mixture of

7 Sn(II)O and Sn(IV)O$_2$ composed in majority of Sn(II)O crystals (Figure 1, Ab). Finally, the alkaline

8 method under mild conditions (75 °C and ambient pressure) produced pure romarchite tetragonal

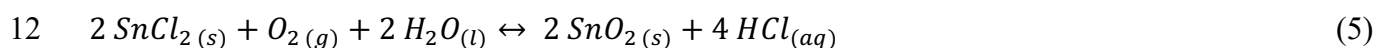9 Sn(II)O (JCPDS card 06-0395) *via* dissolution-precipitation from Sn$_4$(OH)$_6$Cl$_2$ (Figure 1, Ac) [47].
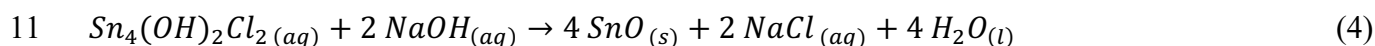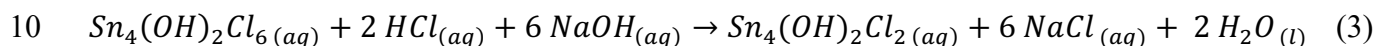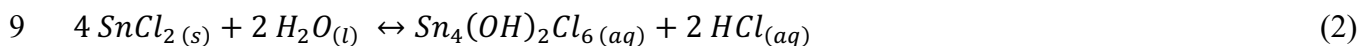
10 However, to maintain Sn in the oxidation state of +2, a minimum amount of NaOH was necessary in

11 order to neutralize the HCl released during the SnCl$_2$ dissolution. Indeed, a detailed investigation on

12 the effect of NaOH concentration revealed that at 0.25 M NaOH (Sn/NaOH = 0.44), the conditions

13 favored maximum formation of cassiterite tetragonal SnO$_2$ (Figure 1, B a), while at 0.38 M (Sn/NaOH

14 = 0.30) (Figure 1, B b) and 0.5 M NaOH (Sn/NaOH = 0.22) (Figure 1, B c), a shiny black solid was

15 recovered, characteristic of tetragonal romarchite Sn(II)O. Notably, the SnO particles prepared with

16 0.38 M NaOH displayed the most intense reflexion peaks of the (001) and (002) facets, located at

17 18.3° and 37.2° respectively, indicating preferential growth of the crystal planes along the (001)

18 direction. However, further increase in the NaOH concentration to 0.75 M (Sn/NaOH = 0.15) was

19 found to be detrimental since it caused total dissolution of the oxide into Na$_2$[Sn(OH)$_6$]$_2$.

Figure 1. XRD patterns of Sn-based oxides prepared by different methods and with different NaOH concentrations. (A) Effect of the preparation method: complexation (a), hydrothermal (b) and alkaline (c). (B) Effect of NaOH concentration on the crystallinity of Sn-based solids prepared by the alkaline method: 0.25 M NaOH (a), 0.38 M NaOH (b) and 0.50 M NaOH (c).

As pointed out by Gulo *et al.*[47], the synthesis of SnO in alkaline media consists of three consecutive reactions: first, $SnCl_2$ is hydrolyzed in water producing $Sn_4(OH)_2Cl_6$ (Equation 2); then, the HCl released is neutralized by the NaOH, while Cl^- ions from $Sn_4(OH)_2Cl_6$ are gradually replaced by hydroxide ions yielding $Sn_4(OH)_6Cl_2$ (Equation 3); finally, the SnO crystals are produced *via* dissolution-precipitation from $Sn_4(OH)_6Cl_2$ during aging at 95°C (Equation 4). Meanwhile, the presence of HCl in the reaction medium, even in small amounts, is likely to promote oxidation of SnO to SnO_2 (Equation 5), consistent with the observation at 0.25 M NaOH.
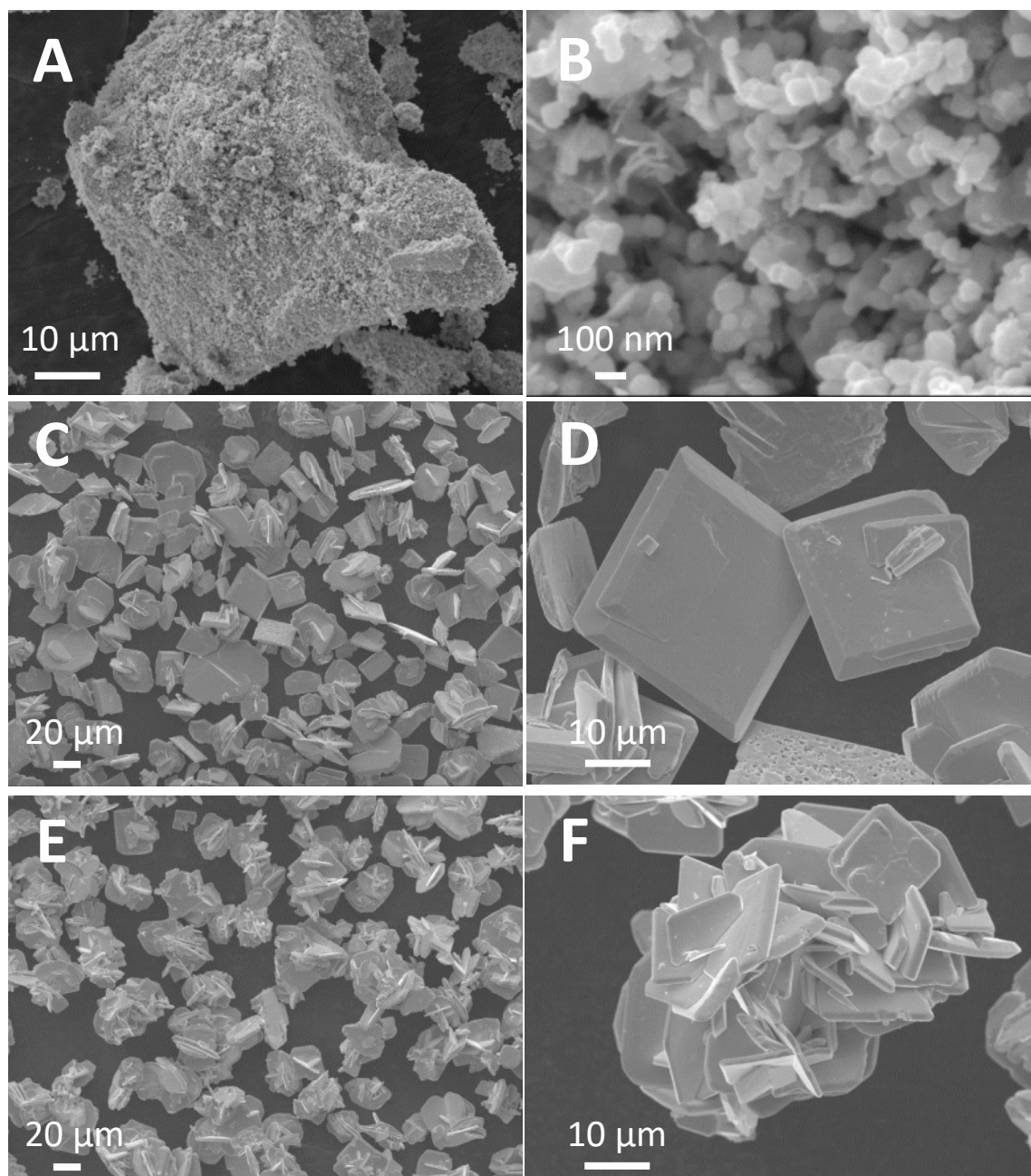
$$4\ SnCl_{2\ (s)} + 2\ H_2O_{(l)} \leftrightarrow Sn_4(OH)_2Cl_{6\ (aq)} + 2\ HCl_{(aq)} \tag{2}$$

$$Sn_4(OH)_2Cl_{6\ (aq)} + 2\ HCl_{(aq)} + 6\ NaOH_{(aq)} \rightarrow Sn_4(OH)_2Cl_{2\ (aq)} + 6\ NaCl_{(aq)} + 2\ H_2O_{(l)} \tag{3}$$

$$Sn_4(OH)_2Cl_{2\ (aq)} + 2\ NaOH_{(aq)} \rightarrow 4\ SnO_{(s)} + 2\ NaCl_{(aq)} + 4\ H_2O_{(l)} \tag{4}$$

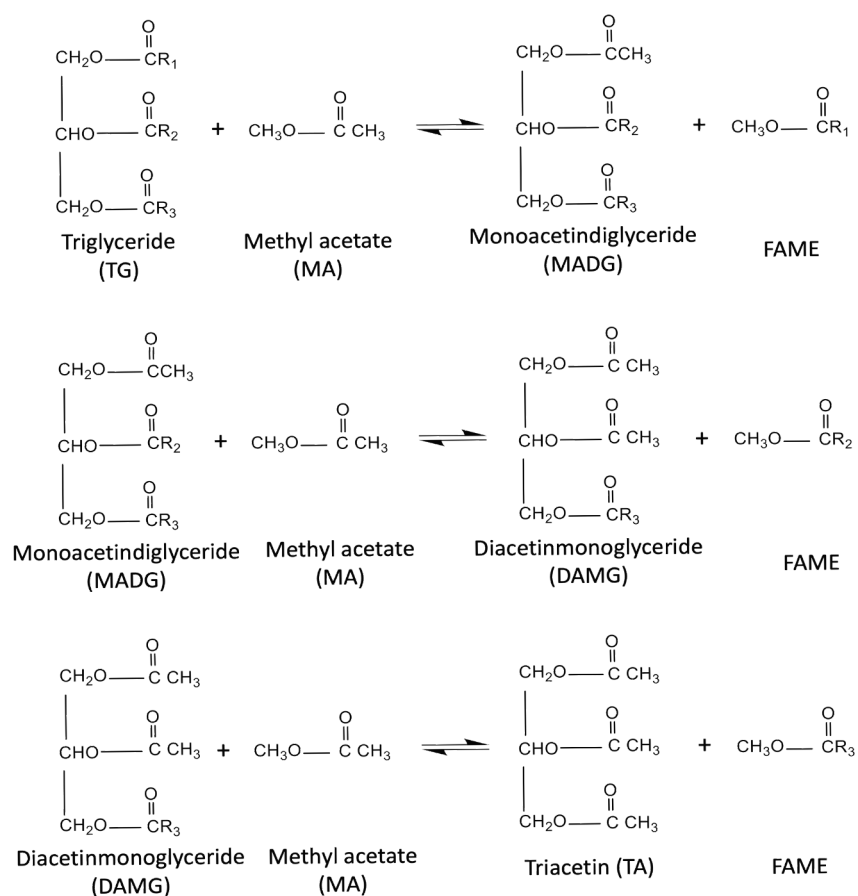$$2\ SnCl_{2\ (s)} + O_{2\ (g)} + 2\ H_2O_{(l)} \leftrightarrow 2\ SnO_{2\ (s)} + 4\ HCl_{(aq)} \tag{5}$$

To gain further insights into the morphological changes on Sn-based crystals with the NaOH concentration, FE-SEM observations were carried out. Representative micrographs revealed a shape evolution from spherical particles to square-plate crystals (Figure 2). Indeed, the Sn-alk-0.25M solid was composed mainly of angular clasts with rough surfaces and irregular boundaries with dimensions ranging from 5 µm to more than 100 µm (Figure 2A, Figure S1 A-C ESI). These clasts consisted mainly of fine-grained and densely-packed spherical particles with smooth surfaces and an average 50-100 nm diameter (Figure 2B, Figure S1 D,E, ESI). Conversely, stacked structures comprised mainly of quadrilateral microplatelets with exposed (001) facets were obtained with the Sn-alk-0.38M catalyst (Figure 2C,D; Figure S2, ESI) in agreement with the XRD data. Microplatelets were about 10-100 µm long and 0.5-2.0 µm thick (Figure S4, ESI). Further increase in the NaOH concentration to 0.5M (Sn-alk-0.50M solid) led to reduction of the average particle sizes to 10-30 µm and to formation of aggregates with 3D flower-like architectures which consisted mainly of interpenetrating

1   micro-sheets (Figure 2E-F, Figure S3, ESI). Noticeably, the (001) facets of Sn-alk-0.50M crystals

2   were less exposed due to the formation of perpendicularly oriented microsheets pointing at different

3   directions, which were at the origin of the attenuation of reflexions at 18.3° and 37.2° in the XRD

4   patterns (Figure 1, B c).

6   **Figure 2.** FEG-SEM micrographs of Sn-based oxides prepared by the alkaline method with different NaOH

7   concentrations: 0.25 M NaOH (A, B), 0.38 M NaOH (C, D) and 0.50 M NaOH (E, F).

1   The catalytic activity of tin-based oxides was evaluated in the interesterification of rapeseed oil using

2   methyl acetate (MA) as acyl donor to produce FAME and triacetin. Most studies show that the

3   interesterification of triglycerides (TG) is a reversible process composed of a sequence of three

4   consecutive second order reversible reactions, involving the formation of monoacetindiglyceride

5   (MADG) and diacetinmonoglyceride (DAMG) intermediates, together with triacetin (TA) (Scheme

6   1) [12,23,32].Stoichiometrically, three molecules of methyl acetate are required to react

7   consecutively with one molecule of triglyceride, producing one molecule of methyl ester (biodiesel)

8   at each step and one molecule of triacetin at the last step. However, in practice, the acyl donor is

9   usually utilized in strong excess with respect to the reaction stoichiometry in order to shift the

10   equilibrium of each step to the right (product side), thus reducing the residual amounts of

11   intermediates.

12
13 **Scheme 1.** Interesterification reaction between a triglyceride and methyl acetate leading to formation of fatty acid methyl

14 esters (FAME) and triacetin (TA) passing through monoacetindiglyceride (MADG) and diacetinmonoglyceride (DAMG)

15 intermediates.

16

1 Indeed, as reported by Casas *et al.* [22], triglycerides can be totally converted using a MA/TG molar

2 ratio of 18. However, a molar ratio of 50 was needed to completely transform the

3 monoacetindiglyceride, while a MA/TG molar ratio as high as 100 was not enough to completely

4 remove the diacetinmonoglyceride. This is a clear indication of the high degree of reversibility of the

5 interesterification reaction where the conversion of diacetinmonoglyceride to triacetin is the rate-

6 limiting step. It is important to point out that, using methyl acetate in large excess is also an effective

7 way to reduce the viscosity of triglycerides and dissolve the monoacetindiglyceride and

8 diacetinmonoglyceride intermediates as well as triacetin [38].

9 In our study, the interesterification reaction was set at 210 °C, using a methyl acetate-to-oil molar

10 ratio (MA/TG) of 40 and a catalyst-to-oil molar ratio (SnO/TG) of 0.65 [39]. The results obtained

11 after 30 minutes of reaction time are presented in Table 1, together with those obtained in a control

12 experiment performed with commercial SnO under the same conditions.

13 Similarly to the experiment carried out without catalyst (entry 1), the activities achieved with the

14 SnO_2-based solids were extremely low giving only 1% (entry 2) and 2% (entry 4) FAME yields for

15 the Sn-CM and the Sn-alk-0.25M catalysts respectively. Moreover, triacetin was found only in form

16 of traces. The catalytic activity was slightly improved with the $SnO-SnO_2$ mixture, reaching 7.4%

17 yield in FAME (entry 3). Noticeably, under identical conditions, pure SnO prepared by the alkaline

18 method displayed the highest performance in this reaction, that was quite similar to that of

19 commercial SnO [39].Indeed, 24.2% yield in FAME and 0.3% yield in TA were reached with the Sn-

20 alk-0.38M catalyst (entry 5), while 17.4% FAME and 0.2% TA were achieved with the Sn-alk-0.50M

21 one (entry 6). Although $Sn(IV)O_2$ has proved to be catalytically active in the transesterification of

22 tryglicerides [52], our results clearly revealed that the $Sn(II)O$ was more suitable for the

23 interesterification reaction. As both SnO-alk-0.38M and SnO-alk-0.50M catalysts had very similar

24 surface areas (<1 m^2/g), the superior interesterification activity of the former probably results from

25 its different crystalline properties, in particular the preferential orientation of crystals along the (001)

26 planes, consistent with XRD analysis (Figure 1, B-b) and FE-SEM observations (Figure 2 C,D).

2 **Table 1.** Catalytic performance of Sn-based catalysts in the interesterification of rapeseed oil.[a]

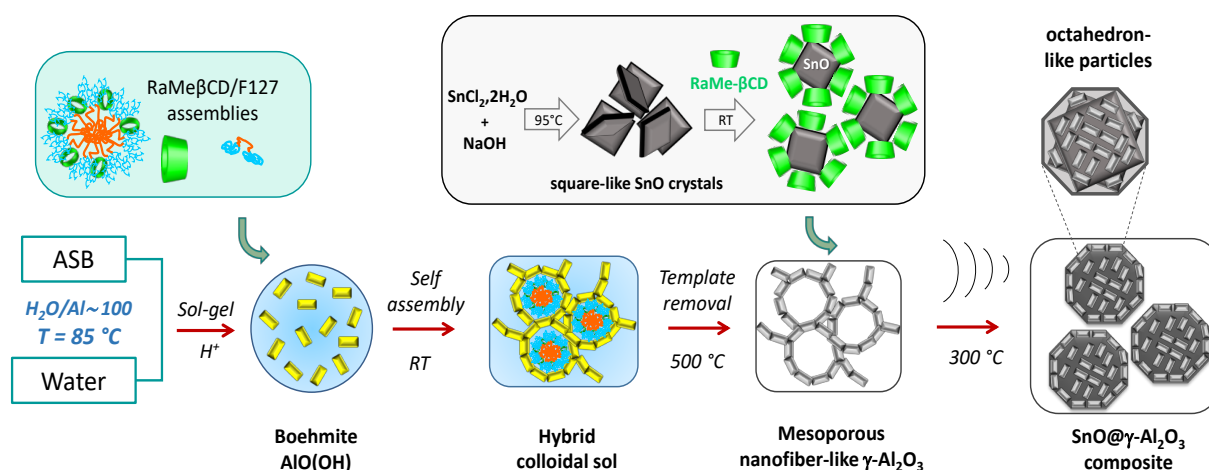| Entry	Catalyst	Crystal phase (XRD)	Interesterification tests	
			Y_{FAME} (w/w %)	Y_{TA} (w/w %)
1	no catalyst	-	0.8	*n.d.*
2	Sn-CM	SnO_2	1.0	n.d.
3	Sn-HT	$SnO-SnO_2$	7.4	n.d.
4	Sn-alk-0.25M	SnO_2	1.22	n.d.
5	Sn-alk-0.38M	SnO	24.2	0.3
6	Sn-alk-0.50M	SnO	17.4	0.2
7	SnO (Alfa Aesar)	SnO	23.6	0.4

3 [a]Reaction conditions: 1.5 g rapeseed oil, 10 wt.% SnO/oil, 5 g methyl acetate (MA/TG = 40), initial pressure inside
4 reactor: 2 bar, vapor pressure MA: 30 bar, temperature 210 °C, reaction time 30 minutes.

5

6 **3.2 Interesterification of rapeseed oil with SnO@γ-Al$_2$O$_3$composites**

7 Encouraged by results obtained with bulk SnO catalystsprepared by the alkaline method and taking

8 into account that they had very low specific surface areas (less than 1 m^2/g) (Table 2), we then decided

9 to disperse SnO particles over a large-pore mesoporous γ-Al$_2$O$_3$matrix prepared by the colloidal

10 approach [48].

11 The procedure used for the preparation of SnO@γ-Al$_2$O$_3$ composites is illustrated in Scheme 2. First,

12 a boehmite (AlO(OH)) sol was synthesized in aqueous phase by sol-gel process at 85 °C using

13 aluminum tri-*sec* butoxide (ASB) as precursor (hydrolysis ratio H$_2$O/Al ~ 100) [48]. Then, boehmite

14 nanoparticles were allowed to self-assemble around the supramolecular template formed between the

15 randomly methylated β-CD (RaMeβCD) and the Pluronic F127. After calcination at 500 °C, a

16 mesoporous nanofiber-like γ-Al$_2$O$_3$ solid was recovered. In parallel, micrometric quadrilateral SnO

17 particles were prepared by dissolution-precipitation in alkaline medium (0.38M NaOH) as previously

18 described, then redispersed in a RaMeβCD aqueous solution (30 mg/mL). The obtained hybrid

19 RaMeβCD@SnO-γ-Al$_2$O$_3$ material was subsequently subjected to ultrasonic irradiation for 15

20 minutes. By varying the γ-Al$_2$O$_3$ loading in the RaMeβCD@SnO suspension, mesoporous SnO@γ-

1   Al$_2$O$_3$ composites with tunable porosity and octahedral-shape crystal structures, which are actually

2   stacks of platelets, were obtained after calcination at 300 °C. In this approach, the RaMeβCD had a

3   two-fold role, *i.e.* it showed a pore expansion effect on the γ-Al$_2$O$_3$ shell covering SnO microcrystals

4   [53,54] and at the same time,it acted as structure directing agent owing to its surface-active properties

5   [43,55] which are beneficial for reducing the surface energy of SnO microcrystals, thus facilitating

6   their co-assembly with γ-Al$_2$O$_3$nanoparticles.
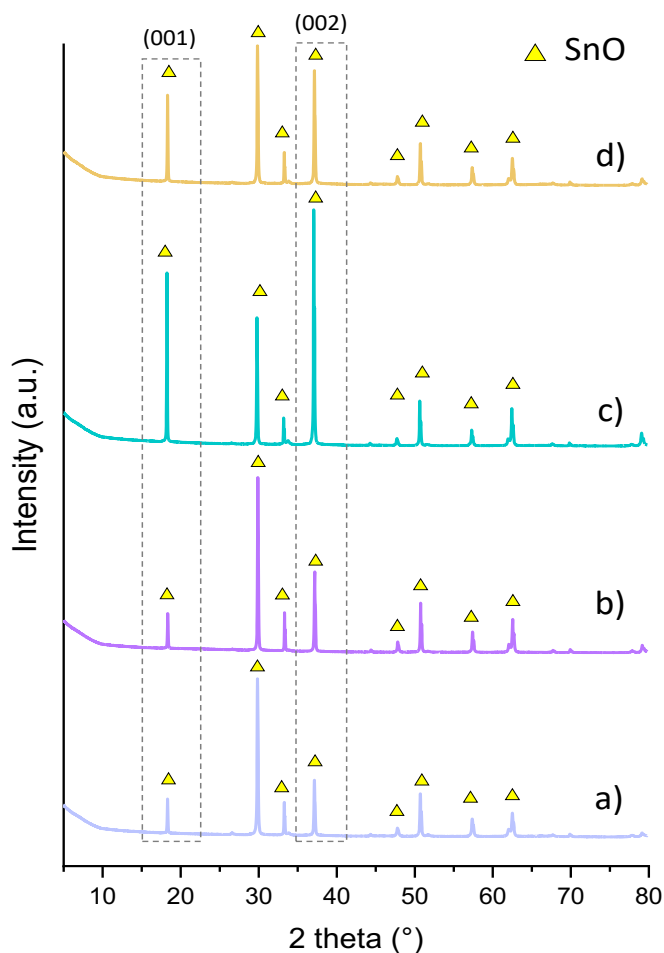

7

8   **Scheme 2.** Schematic illustration of the procedure used for the preparation method of SnO@γ-Al$_2$O$_3$ composites.

9   From the TEM images (Figure S5 A,B, ESI), it can be seen that, in a contrast to the template-free sol-

10   gel γ-Al$_2$O$_3$, the morphology of RaMeβCD-templated γ-Al$_2$O$_3$ was fibber-like and the entanglement

11   of alumina fibbers produced nanometric voids with an average diameter of 11.2 nm (Figure S5 C,

12   ESI). Such evolution in the γ-Al$_2$O$_3$particle morphology was at the origin of the increase in the surface

13   area (from 219 to 236 m^2/g), pore size (from 4.2 to 11.2 nm) and pore volume (from 0.276 to 0.674

14   cm^3/g) (Table 2), which can be correlated to the ability of RaMeβCD to act as micelle expander

15   [53,54]. XRD analysis also confirmed that the temperature of 500°C was sufficient to totally convert

16   boehmite to γ-Al$_2$O$_3$ (Figure S5 D, ESI).

17   To investigate the impact of RaMeβCD-templated γ-Al$_2$O$_3$ particles on the structural, textural and

18   morphological characteristics of SnO@γ-Al$_2$O$_3$ composites, X-ray diffraction (XRD), N$_2$-adsorption

19   and field emission gun scanning electron microscopy (FE SEM) analyses were carried out.

1 XRD patterns (Figure 3) revealed that the intensity of (001) and (002) peaks was greatly enhanced

2 upon increasing the γ-Al$_2$O$_3$ loading, indicating that alumina can modulate the orientation growth of

3 SnO crystals in a direction parallel to the (001) plane. Indeed, it is possible that γ-Al$_2$O$_3$ particles

4 adsorb preferentially on the (001) facets of SnO, which are actually the most thermodynamically

5 stableand possess the lowest surface energy [56]. Such adsorption could facilitate stacking of SnO

6 crystals and promote their growth into polyhedral-shaped particles with well-developed (001) facets.

7 Note that among the four catalysts, SnO@γ-Al$_2$O$_3$1.0 prepared with an equimolar Sn/Al composition

8 showed the highest reflexion intensities at 18.3° and 37.2° indicative of development of structures

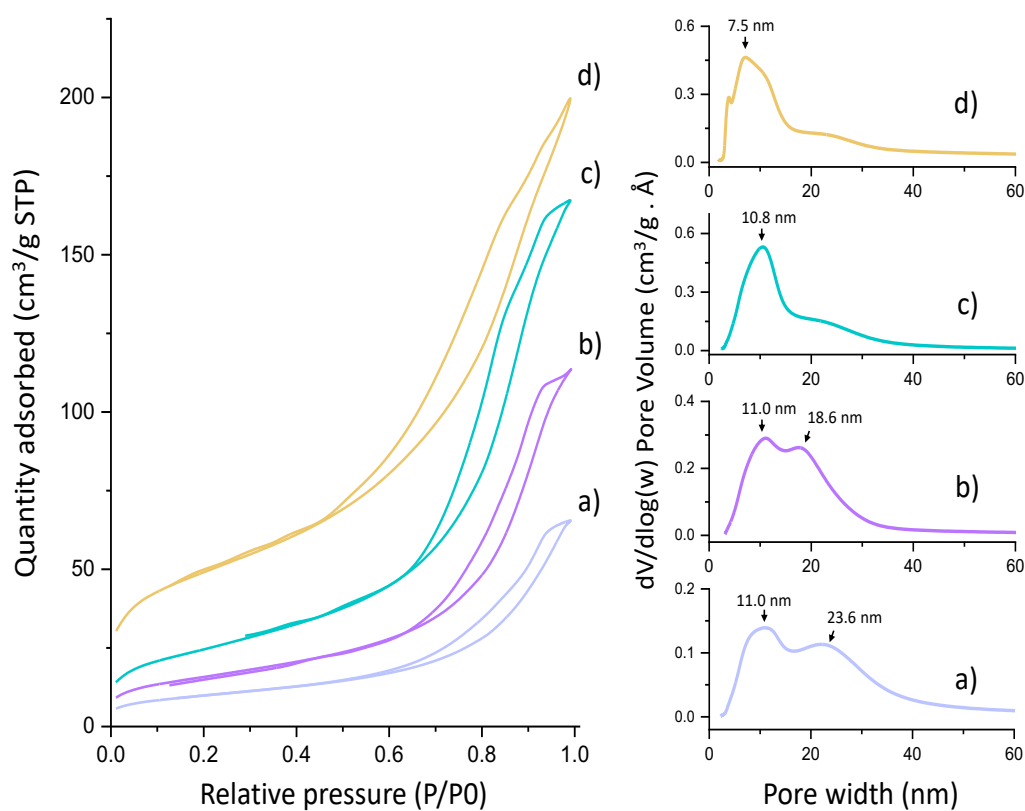9 with most abundant exposed (001) facets.

10

11 **Figure 3.** XRD patterns of SnO@γ-Al$_2$O$_3$ composites: (a) SnO@γ-Al$_2$O$_3$0.5, (b) SnO@γ-Al$_2$O$_3$0.67, (c) SnO@γ-

12 Al$_2$O$_3$1.0, (d) SnO@γ-Al$_2$O$_3$2.0.

13

From the N_2-adsorption analysis (Figure 4), it can be seen that all SnO@γ-Al$_2$O$_3$ composites displayed type-IV isotherms with a type H3 hysteresis loop, characteristic of mesoporous materials with wide pore size distributions. As a general trend, upon increasing the γ-Al$_2$O$_3$ loading, a significant increase in the specific surface area (from 35 to 173 m^2/g) and pore volume (from 0.103 to 0.307 cm^3/g) was noticed. Bimodal pore size distributions were developed for the composites prepared with the lowest Al/Sn molar ratios, while monomodal structures were obtained for the highest alumina loadings. The largest pores with an average diameter of 19-24 nm probably resulted from the high degree of freedom of γ-Al$_2$O$_3$nanoparticles deposited on the surface of SnO microcrystals, enabling the formation of a fibrous network, while the smallest ones (9-11 nm) were characteristic of bare γ-Al$_2$O$_3$with a higher degree of particle aggregation (Figure S5, ESI). This means that in our composites, γ-Al$_2$O$_3$ particles are either assembled into fibbers or densely packed in more compact structures,on the surface of the SnO crystals, as aggregates.

Figure 4. N_2 adsorption isotherms (A) and corresponding pore size distributions (B) of SnO@γ-Al$_2$O$_3$ composites: (a) SnO@γ-Al$_2$O$_3$0.5, (b) SnO@γ-Al$_2$O$_3$0.67, (c) SnO@γ-Al$_2$O$_3$1.0, (d) SnO@γ-Al$_2$O$_3$2.0.

Table 2. Structural and textural characteristics of γ-Al$_2$O$_3$ supports and SnO@γ-Al$_2$O$_3$ composites after thermal treatment at 300 °C.

Sample	XRD	N$_2$-adsorption		
		S_{BET}^a (m^2/g)	V_p^b (cm^3/g)	D_p^c (nm)
Sol-gel γ-Al$_2$O$_3$	γ-Al$_2$O$_3$	219	0.276	4.2
γ-Al$_2$O$_3$	γ-Al$_2$O$_3$	236	0.674	11.2
Sn-alk-0.38M	SnO	<1	nd	nd
SnO@γ-Al$_2$O$_3$0.5	SnO	35	0.103	11.0/23.6
SnO@γ-Al$_2$O$_3$0.75	SnO	56	0.174	11.0/18.6
SnO@γ-Al$_2$O$_3$1.0	SnO	88	0.261	10.8
SnO@γ-Al$_2$O$_3$2.0	SnO	173	0.307	7.5

[a]specific surface area determined in the relative pressure range 0.1-0.25, [b]cumulative pore volume and [c]averagepore diameter resulting from BJH calculations.

Evidence for the shape evolution from squares (bare SnO) to truncated octahedral-like particles (SnO@γ-Al$_2$O$_3$composites) was provided by FE-SEM observations, which confirmed that γ-Al$_2$O$_3$ nanoparticles assembled almost exclusively on the surface of SnO promoting the growth of microcrystals in a direction parallel to the (001) plane (Figures S6-S10, ESI). Representative FE-SEM images of the SnO@γ-Al$_2$O$_3$1.0 composite (Figure 5) indicated that this solid was composed mainly of individual non-aggregated structures with octahedral shapes and smooth boundaries (Figure 5 A-D) having a typical length of 20 to 30 µm and a thickness of about 2 µm (Figure 5 E-F). EDX elemental mapping (Figure 5 G) also confirmed that Al, O and Sn atoms were uniformly distributed on the microplatelets. Locally, some aggregation of alumina nanoparticles was also observed on the surface of SnO microcrystals. It is worth noting that those composite particles also presented some surface damages due to partial eradication of SnO crystals caused by the ultrasonic irradiation, which resulted in formation of holes in the center of the polyhedra and, in some cases, fragmentation of the crystals. Nevertheless, upon increasing the γ-Al$_2$O$_3$ loading, this phenomenon was attenuated, consistent with the increase in the plate thickness, thus providing greater improvement of the impact resistance (Figures S6-S10, ESI).

Figure 5. FE-SEM images (A-F) of SnO@γ-Al$_2$O$_3$1.0 composite and corresponding EDX elemental mapping distribution of Al, O, Sn and C (G).

1   The catalytic activity of SnO@γ-Al₂O₃ composites was then evaluated in the interesterification of

2   rapeseed oil under the same conditions as with bare SnO. FAME and triacetin yields obtained with

3   the different supported catalysts are shown in Table 3. Clearly, the overall activity was dependent on

4   the γ-Al₂O₃ loading. While mesoporous γ-Al₂O₃ was almost inactive after 30 min at 210°C (entry 1),

5   the addition of a small amount of γ-Al₂O₃ to the SnO catalyst (Al/Sn molar ratio = 0.5) resulted in an

6   increase in the FAME yield to 24.9% (entry 3), which represents, however, only a slight improvement

7   (by ~0.7%) with respect to bare SnO (entry 2). As shown previously by several authors, γ-Al₂O₃ may

8   catalyze efficiently interesterification of triglycerides, however, higher temperatures and pressures

9   are required compared to our conditions. Indeed, Ribeiro *et al.*[36] obtained 82.5% conversion

10   efficiency with macaw oil using γ-Al₂O₃ as catalyst at a temperature of 300 °C under autogenous

11   pressure, while a 60.2% FAME yield was reported by Visioli *et al.* [57] at a temperature of 275°C

12   and 20 MPa pressure. Interestingly, we noticed cooperative effects upon increasing the γ-Al₂O₃

13   loading, which not only resulted in increased conversion of rapeseed oil, but also promoted the

14   reaction of monoacetindiglyceride and diacetinmonoglyceride intermediates with methyl acetate

15   towards triacetin formation (entries 4-6). As reported in many studies [9,12,23,58], triacetin can be

16   used as a fuel additive or included in the biodiesel formulation up to 10 wt % since it enhances the

17   biodiesel quality. However, above this limit threshold, it tends to reduce the cetane number of

18   biodiesel below the minimum limit fixed by the EN 14214 guidelines [9]. The FAME yields obtained

19   with our catalysts after 30 minutes at 210 °C were 27.2% for SnO@Al₂O₃0.75 (entry 4), 30.9% for

20   SnO@Al₂O₃1.0 (entry 5) and 33.5% for SnO@Al₂O₃2.0 (entry 6), giving triacetin yields of 1.0%,

21   2.0% and 1.5% respectively.

22   Among the different composites, SnO@Al₂O₃ 2.0 appeared to be the most suitable for rapeseed

23   biodiesel production, achieving a global yield of 35.0% after 30 minutes and 82.5 % after 120 minutes

24   (Figure S11, ESI). Interestingly, this catalyst was also more active than the commercial SnO (entry

25   7). Time course analysis (Figure S11, ESI) also indicated that the reaction kinetics were faster with

1     $SnO@Al_2O_32.0$, showing almost 10 wt.% differences in FAME yields on consecutive 30-min time

2   intervals.

3   Based on the characterization results, it is clear that the catalytic performance of $SnO@\gamma-Al_2O_3$

4   composites results from a combined effect of textural, structural and morphological characteristics.

5   Thus, the largest surface area obtained with $SnO@\gamma-Al_2O_32.0$ catalyst (173 m^2/g) should provide a

6   greater number of adsorption sites and active centers, facilitating the adsorption properties of the

7   composite towards both triglycerides and methyl acetate. Moreover, its high pore volume (0.307

8   cm^3/g) should improve the diffusion of both reactants and products during the catalytic process and

9   reduce the mass transfer limitations, which are critical issues for microporous catalysts. Finally, the

10   mesoporous $\gamma-Al_2O_3$material can also modify or reshape the SnO microcrystals and promote their

11   growth along the (001) planes, which appear to be the most active in the interesterification reaction.

12   Overall, these results showed that $\gamma-Al_2O_3$ may be a suitable material for preparing SnO-based

13   composites with enhanced interesterification activities; however, when this oxide was used in a large

14   excess to SnO (Al/Sn molar ratio of 2.0) a drop in TA yield was also observed (from 2.0% to1.5%),

15   which is probably due to parallel undesired decomposition reactions catalyzed by the alumina-

16   enriched composite [37].

17   Our results can be compared with those of Nunes and Castilhos [59] who obtained 62.3 wt.% FAME

18   yield in the interesterification of soybean oil with methyl acetate using calcium oxide (CaO) as

19   heterogeneous catalyst. The optimum conditions found by the authors were a MA:oil molar ratio of

20   40:1, 10 wt.% catalyst, 325°C temperature and 4 hours reaction time. In addition, the authors found

21   that CaO was the most efficient catalyst in comparison with Y-zeolite, MgO, Nb_2O_5 and mixed oxides

22   [37].

23   It is generally reported that high water concentration in the reaction mixture decreases the activity of

24   homogeneous and heterogeneous catalysts preventing the utilization of cheap feedstocks, such as

25   waste cooking oil [60].To this end, the $SnO@\gamma-Al_2O_32.0$ composite was selected to investigate the

effect of water as impurity. An additional run was performed under the same operating conditions as in the preceding experiments, with the only exception that 2 wt.% water was deliberately added in the reaction medium.

Table 3. Catalytic performance of Sn-based catalysts in the interesterification of rapeseed oil to biodiesel and triacetin.[a]
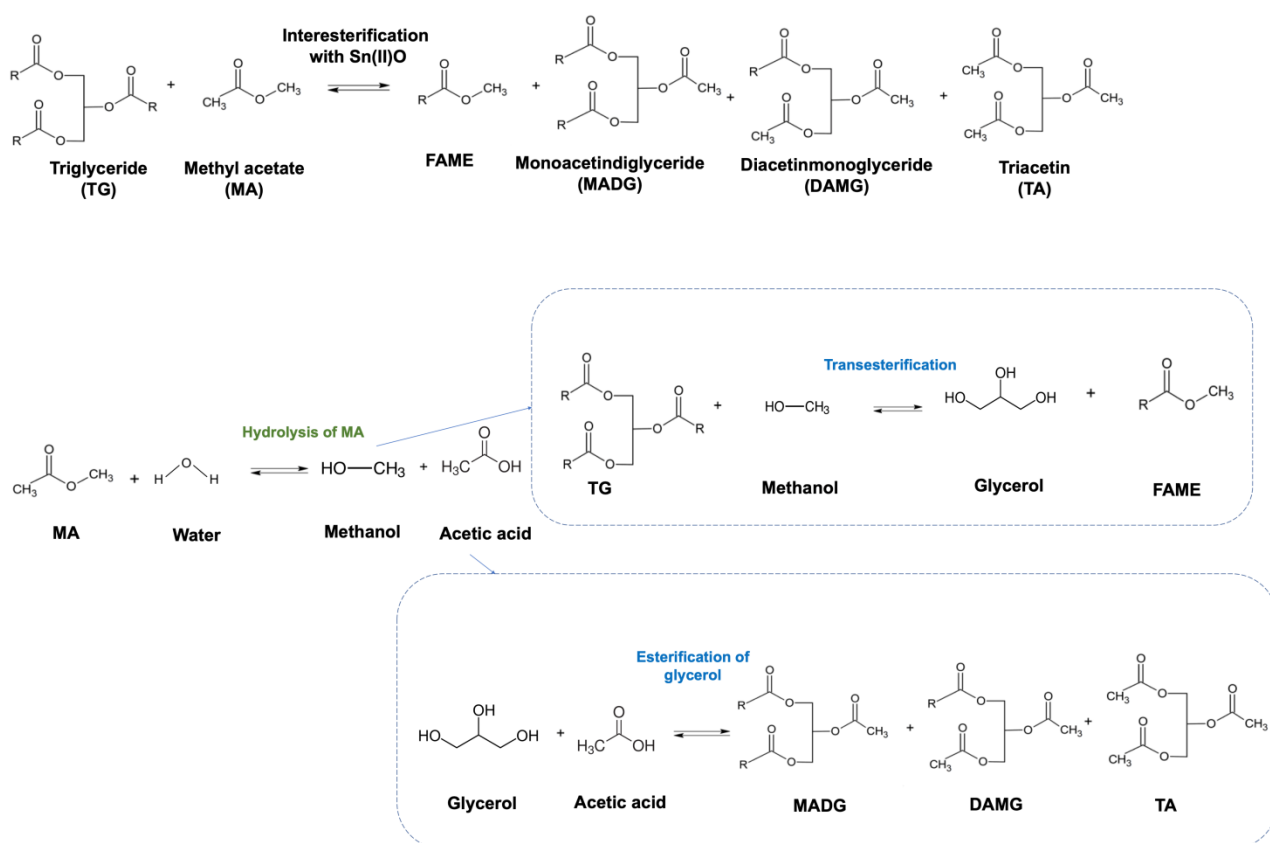
Entry	Catalyst	Interesterification tests	
		Y_{FAME} (w/w %)	Y_{TA} (w/w %)
1	Mesoporous γ-Al_2O_3	2.0	n.d.
2	SnO-alk-0.38M	24.2	0.3
3	SnO@$Al_2O_3$0.5	24.9	n.d.
4	SnO@$Al_2O_3$0.75	27.2	1.0
5	SnO@$Al_2O_3$1.0	30.9	2.0
6	SnO@$Al_2O_3$2.0	33.5	1.5
7	SnO-comm (Alfa Aesar)	23.6	0.4
8	SnO@$Al_2O_3$2.0-water	47.5	2.4

[a]Reaction conditions: 1.5 g rapeseed oil, 10 wt.% SnO/oil, 5 g methyl acetate (MA/TG = 40), initial pressure inside reactor: 2 bar, vapor pressure MA: 30 bar, temperature 210 °C, reaction time 30 minutes.

We noticed that FAME and TA yields were greatly enhancedupon addition of water, reaching 47.5% and 2.4% respectively (entry 8,Table 3),thus reproducingthe behavior obtained with commercial bulk SnO [39]. Such effect could be related to a possible modification of the reaction mechanism, where interesterification, transesterification and esterification reactions could be combined in a consecutive continuous process. Indeed, as illustrated in Scheme 3, in the presence of water, SnO may catalyze first the hydrolysis of methyl acetate to acetic acid and methanol, then this latter may react with triglycerides through a transesterification reaction yielding glycerol and FAME. In parallel, glycerol could also react with acetic acid through an esterification reaction yielding triacetin, diacetinmonoglyceride and monoacetindiglyceride.

As pointed out by Casas *et al.*[22], transesterification has faster kinetics when compared to interesterification since it uses methanol as acyl receptor, which usually requires milder conditions to achieve higher yields. Farobie and Matsumura [61] have explained this difference by the lower reactivity of supercritical methyl acetate producing an unstable intermediate, which requires higher
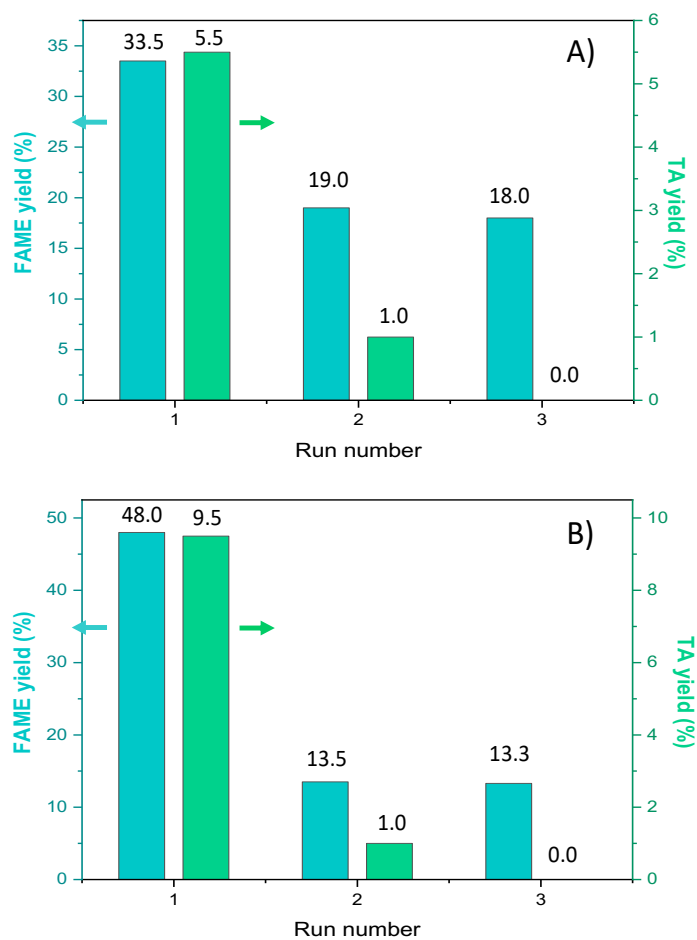
1 activation energy when compared to supercritical methanol. Supporting evidence in favor of the

2 proposed mechanism was provided by the chromatographic profiles (Figure S12, ESI), where the

3 ratio of the peak areas corresponding to diacetinmonoglyceride and monoacetindiglyceride increased

4 with respect to the internal standard peak upon addition of 2 wt.% water in the reaction medium. In

5 contrast, in the absence of added water, those ratios were very low, suggesting the formation of only

6 traces of MADG and DAMG.

7
8 **Scheme 3.** Schematic illustration of biodiesel production in the presence of methyl acetate (MA) and water by

9 simultaneous interesterification and transesterification.

10 An important issue in the perspective of utilization of heterogeneous catalysts in industrial application

11 is their long term stability. To assess this aspect we evaluated the recyclability of SnO@γ-Al$_2$O$_3$2.0

12 under the same reaction conditions (MA/TG molar ratio of 40, a catalyst content of 10 wt.%, and a

13 reaction temperature of 210°C for 30 minutes). The FAME and triacetin yields obtained during the

14 reuse tests, with and without water, are shown in Figure 6. In the absence of water, FAME content

15 decreased from 33.5 % in the first run to 19.0% in the second run and then was stabilized to 18.0%

1   in the third run, representing a catalytic efficiency decay of 45.6% (Figure 6, A).However, in the

2   presence of 2 wt.% water, a more pronounced catalytic efficiency loss (72.3 %)was observed (Figure

3   6, B). We identified that washing the catalyst with methyl acetate between consecutive runs did not

4   produced any significant improvement in the catalytic activity (Figure S13, ESI), therefore excluding

5   a possible blockage of catalyst active sites by the reactants. One of the factors at the origin of such

6   activity decay may be the instability of γ-Al_2O_3 under our reaction conditions, especially in the

7   presence of water [62,63]. Indeed, the XRD diagram of the catalyst recovered after the third run in

8   the experiment conducted with 2 wt.% water showed that tin was still in the oxidation state +2, but

9   γ-Al_2O_3 was hydrolyzed into boehmite (Figure S14, ESI). Such a transformation would probably be

10 accelerated by the acetic acid formed during the hydrolysis of methyl acetate, implying partial

11 dissolution of the support and loss of a part of catalyst particles. Despite that decay, the activities

12 obtained in the third run are still higher than some reported in literature in interesterification reaction

13 with other heterogeneouscatalysts,such as Nb_2O_5 and Y zeolite as well as Mg-Al and Ca-Mg-Al

14 mixed oxides, tested at a temperature similar to that used in our study [37].

Figure 6. Catalytic recyclability of SnO@γ-Al$_2$O$_3$2.0 catalyst in the absence (A) and in the presence of 2 wt.% water (B). Reaction conditions: 1.5 g rapeseed oil, 10 wt.% SnO/oil, 5 g methyl acetate (MA/substrate = 40), initial pressure inside reactor: 2 bar, vapor pressure MA: 30 bar, temperature 210 °C, reaction time 30 minutes.

Conclusions

In summary, pure romarchite tetragonal Sn(II)O, prepared under alkaline conditions at 75 °C *via* dissolution-precipitation from Sn$_4$(OH)$_6$Cl$_2$,was found to be more suitable catalyst in the interesterification of rapeseed oil with methyl acetate with respect to the cassiterite tetragonal Sn(IV)O$_2$ and the Sn(II)O/Sn(IV)O$_2$ mixture, achieving 24.2 % yield in FAME after 30 minutes at 210 °C. To further improve the morphological and surface properties of Sn(II)O, mesoporous Sn(II)O@γ-Al$_2$O$_3$ core-shell octahedral composites were prepared through a hierarchical self-assembly process triggered by randomly methylated β-cyclodextrin (RaMeβCD)-based assemblies. In this approach, RaMeβCD can regulate the orientation of rod-like γ-Al$_2$O$_3$ nanoparticles on the

surface of pre-synthesized micron-size Sn(II)O crystals yielding mesoporous composites with unique properties. Particulate composites were composed of a functional SnO microcrystal core with high catalytic activity and a mesoporous alumina shell with good pore accessibility. Importantly, the γ-Al_2O_3 shell was found to promote stacking of square-like SnO particles along the (001) direction and resulted in formation of single octahedron-like crystals with highly exposed facets that were particularly active in the interesterification of rapeseed oil with methyl acetate. The best results were obtained with the composite prepared with an Al/Sn molar ratio of 2.0 achieving a total FAME and triacetin yield of 35.0% after 30 minutes and 82.5 % after 120 minutes at 210 °C.This novel approach based on γ-Al_2O_3-controlled growth of SnO microcrystals assisted by RaMeβCD provides a brand new way to construct functional composites with new architectures and improved catalytic performance in interesterification reactions.

Appendix A. Supplementary Material

FE-SEM images of bare SnO and SnO@γ-Al_2O_3 composites, kinetics of interesterification of rapeseed oil with methyl acetate catalyzed by the SnO@γ-$Al_2O_3$2.0 composite, chromatographic profiles of reaction products, catalytic recyclability of SnO@γ-Al_2O_3 with intermittent washing between runs, XRD patterns of SnO@γ-$Al_2O_3$2.0 after catalytic test in 2 wt.% water.

1 **References**
2

[1] A.O. Esan, O.M. Olabemiwo, S.M. Smith, S. Ganesan, A concise review on alternative route of biodiesel production via interesterification of different feedstocks. Int. J. Energy Res. 45 (2021) 12614-12637. https://doi.org/10.1002/er.6680

[2] S.H. Liu, Y.C. Lin, K.H. Hsu, Emissions of regulated pollutants and PAHs from waste- cooking-oil biodiesel-fuelled heavy-duty diesel engine with catalyser, Aerosol Air Qual. Res. 12 (2012) 218-227. https://doi.org/10.4209/aaqr.2011.09.0144

[3] C.Y. Lin, H.A. Lin, L.B. Hung, Fuel structure and properties of biodiesel produced by the peroxidation process, Fuel 85 (2006) 1743-1749. https://doi.org/10.1016/j.fuel.2006.03.010

[4] C.C. Enweremadu, M.M. Mbarawa, Technical aspects of production and analysis of biodiesel from used cooking oil. A review, Renew. Sust. Energ. Rev. 13 (2009) 2205-2224. https://doi.org/10.1016/j.rser.2009.06.007

[5] S.V. Ranganathan, S.L. Narasimhan, K. Muthukumar, An overview of enzymatic production of biodiesel, Bioresour. Technol. 99 (2008) 3975-3981, https://doi.org/10.1016/J.Biortech.2007.04.060.

[6]R. Estevez, L. Aguado-Deblas, F.M. Bautista, D. Luna, Luna, C.; J. Calero, A. Posadillo, A.A. Romero, Biodiesel at the Crossroads: A Critical Review. Catalysts 9 (2019) 1033. https://doi.org/10.3390/catal9121033

[7] A. Abbaszaadeh, B. Ghobadian, M.R. Omidkhah, G. Najafi, Current biodiesel production technologies: A comparative review. Energy Convers. Manag. 63 (2012) 138-148. https://doi.org/10.1016/j.enconman.2012.02.027

[8] A. Casas, M.J. Ramos, Á. Pérez, Methanol-enhanced chemical interesterification of sunflower oil with methyl acetate, Fuel 106 (2013) 869-872. https://doi.org/10.1016/j.fuel.2012.11.037

[9] A. Casas, J. R. Ruiz, M. J. Ramos, A. Perez, Effects of triacetin on biodiesel quality, Energy Fuels 24 (2010) 4481-4489. https://doi.org/10.1021/ef100406b

[10] M.E. Borges, L. Díaz, Recent developments on heterogeneous catalysts for biodiesel production by oil esterification and transesterification reactions: a review, Renew. Sust. Energ. Rev. 16 (2012) 2839-2849. https://doi.org/10.1016/j.rser.2012.01.071

[11] P. Campanelli, M. Banchero, L. Manna, Synthesis of biodiesel from edible, non-edible and waste cooking oils via supercritical methyl acetate transesterification, Fuel 89 (2010) 3675-3682. https://doi.org/10.1016/j.fuel.2010.07.033

[12] S. Saka, Y. Isayama, A new process for catalyst-free production of biodiesel using supercritical methyl acetate, Fuel 88 (2009) 1307-1313. https://doi.org/10.1016/j.fuel.2008.12.028

[13] F. Goembira, K. Matsuura, S. Saka, Biodiesel production from rapeseed oil by various supercritical carboxylate esters, Fuel 97 (2012) 373-378. https://doi.org/10.1016/j.fuel.2012.02.051

[14] F. Goembira, S. Saka, Advanced supercritical methyl acetate method for biodiesel production from Pongamia pinnata oil, Renew. Energy 83 (2015) 1245-1249. https://doi.org/10.1016/j.renene.2015.06.022

[15] F. Goembira, S. Saka, Factors affecting biodiesel yield in interesterification of rapeseed oil by supercritical methyl acetate, Green Energy Technol. 108 (2012) 147-152. https://doi.org/10.3390/pr9010138

[16] N. Sootchiewcharn, L. Attanatho, P. Reubroycharoen, Biodiesel production from refined palm oil using supercritical ethyl acetate in a microreactor, Energy Procedia. 79 (2015) 697-703. https://doi.org/10.1016/j.egypro.2015.11.560

[17] W. Sakdasri, S. Ngamprasertsith, S. Daengsanun, R. Sawangkeaw, Lipid-based biofuel synthesized from palm-olein oil by supercritical ethyl acetate in fixed-bed reactor, Energy Convers. Manag. 182 (2019) 215-223. https://doi.org/10.1016/j.enconman.2018.12.041

[18] Z. Abelniece, L. Laipniece, V. Kampars, Biodiesel production by interesterification of rapeseed oil with methyl formate in presence of potassium alkoxides. Biomass Conv. Bioref. (2020). https://doi.org/10.1007/s13399-020-00874-z

[19] V. Kampars, Z. Abelniece, K. Lazdovica, R. Kampare, Interesterification of rapeseed oil with methyl acetate in the presence of potassium tert-butoxide solution in tetrahydrofuran, Renewable Energy 158 (2020) 668-674. https://doi.org/10.1016/j.renene.2020.04.044

[20] V. Kampars, Z. Abelniece, S. Blaua, The Unanticipated Catalytic Activity of Lithium tert-Butoxide/THF in the Interesterification of Rapeseed Oil with Methyl Acetate, J. Chem. 2019 (2019). https://doi.org/10.1155/2019/1509706

[21] A. M. Medeiros, E. R. M. Santos, S. H. G. Azevedo, A. A. Jesus, H. N. M. Oliveira, E. M. B. D. Sousa, Chemical interesterification of cotton oil with methyl acetate assisted by ultrasound for biodiesel production. Brazilian J. Chem. Eng. 3 (2018) 1005-1018. https://doi.org/10.1590/0104-6632.20180353s20170001

[22] A. Casas, M.J. Ramos, A. Pérez, Kinetics of chemical interesterification of sunflower oil with methyl acetate for biodiesel and triacetin production, Chem. Eng. J. 171 (2011) 1324-1332. https://doi.org/10.1016/j.cej.2011.05.037

[23] A. Casas, M.J. Ramos, A. Pérez, New trends in biodiesel production: chemical interesterification of sunflower oil with methyl acetate, Biomass Bioenergy 35 (2011) 1702-1709. https://doi.org/10.1016/j.biombioe.2011.01.003

[24] I. Miesiac, A. Rogalinski, P. Jozwiak, Transesterification of triglycerides with ethyl acetate, Fuel 105 (2013) 169-175. https://doi.org/10.1016/j.fuel.2012.06.086

[25] R.D. Kusumaningtyas, R. Pristiyani, H. Dewajani, A new route of biodiesel production through chemical interesterification of jatropha oil using ethyl acetate, Int. J. Chem Tech. Res. 9 (2016) 627-634. https://sphinxsai.com/2016/ch_vol9_no6/3/(627-634)V9N6CT.pdf

[26] A. Galia, A. Centineo, G. Saracco, B. Schiavo, O. Scialdone, Interesterification of rapeseed oil catalyzed by tin octoate, Biomass Bioenergy 67 (2014) 193-200. https://doi.org/10.1016/j.biombioe.2014.04.025

[27] R. Dicosimo, J. McAuliffe, A.J. Poulose, G. Bohlmann, Industrial use of immobilized enzymes, Chem. Soc. Rev. 42 (2013) 6437-6474. https://doi.org/10.1039/C3CS35506C

[28] E. Jenab, F. Temelli, J.M. Curtis, Y.Y. Zhao, Performance of two immobilized lipases for interesterification between canola oil and fully-hydrogenated canola oil under supercritical carbon dioxide, LWT Food Sci. Technol. 58 (2014) 263-271. https://doi.org/10.1016/j.lwt.2014.02.051

[29] C. Pacheco, C. Palla, G.H. Crapiste, M.E. Carrín, Optimization of reaction conditions in the enzymatic interesterification of soybean oil and fully hydrogenated soybean oil to produce plastic fats, J. Am. Oil Chem. Soc. 90 (2013) 391-400. https://doi.org/10.1007/s11746-012-2182-z

[30] B. Bharathiraja, J. Jayamuthunagai, R. Praveenkumar, M. Jayakumar, S. Palani, The kinetics of interesterfication on waste cooking oil (sunflower oil) for the production of fatty acid alkyl esters using a whole cell biocatalyst (Rhizopus oryzae) and pure lipase enzyme, Int. J. Green Energy 12 (2015) 1012-1017. https://doi.org/10.1080/15435075.2014.882339

[31] J.S. Mendes, J.S. Silva, A.L.O. Ferreira, G.F. Silva, Simulation of process inter- esterification in fluidized bed bioreactor for production of biodiesel, Comput. Aided Chem. Eng. 27 (2009) 1803-1808. https://doi.org/10.1016/S1570-7946(09)70691-1

[32] Y. Xu, W. Du, D. Liu, Study on the kinetics of enzymatic interesterification of triglycerides for biodiesel production with methyl acetate as the acyl acceptor, J. Mol. Catal. B: Enzymatic 32 (2005) 241-245. https://doi.org/10.1016/j.molcatb.2004.12.013.

[33] W. Du, Y. Xu, D. Liu, J. Zeng, Comparative study on lipase-catalyzed transformation of soybean oil for biodiesel production with different acyl acceptors, J. Mol. Catal. B Enzym. 30 (2004) 125-129, https://doi.org/10.1016/j.molcatb.2004.04.004.

[34] E.M. Usai, M.F. Sini, D. Meloni, V. Solinas, A. Salis, Sulfonic acid-functionalized mesoporous silicas: microcalorimetric characterization and catalytic performance toward biodiesel synthesis, Microporous Mesoporous Mater. 179 (2013) 54 - 62. http://dx.doi.org/10.1016/j.micromeso.2013.05.008

[35] J. S. Ribeiro, D. Celante, S.S. Simões, M.M. Bassaco, C. da Silva, F. de Castilhos, Efficiency of heterogeneous catalysts in interesterification reaction from macaw oil (Acrocomia aculeata) and methyl acetate, Fuel 200 (2017) 499-505. https://doi.org/10.1016/j.fuel.2017.04.003

[36] J. S. Ribeiro, D. Celante, L. N. Brondani, D.O. Trojahn, C. Da Silva, F. De Castilhos, Synthesis of methyl esters and triacetin from macaw oil (Acrocomia aculeata) and methyl acetate over γ-alumina, Ind. Crops. Prod. 124 (2018) 84-90. https://doi.org/10.1016/j.indcrop.2018.07.062

[37] S. S. Simões, J. S. Ribeiro, D. Celante, L. N. Brondani, F. Castilhos, Heterogeneous catalyst screening for fatty acid methyl esters production through interesterification reaction, Renewable Energy 146 (2020) 719-726. https://doi.org/10.1016/j.renene.2019.07.023

[38] M. S. Dhawan, S. Calabrese Barton, G. D. Yadav, Interesterification of triglycerides with methyl acetate for the co-production biodiesel and triacetin using hydrotalcite as a heterogenous base catalyst, Catal. Today 375 (2021) 101-111, https://doi.org/10.1016/j.cattod.2020.07.056.

[39] L. Interrante, S. Bensaid, C. Galletti, R. Pirone, B. Schiavo, O. Scialdone, A. Galia, Interesterification of rapeseed oil catalysed by a low surface area tin (II) oxide heterogeneous catalyst, Fuel Process. Technol. 177 (2018) 336-344. https://doi.org/10.1016/j.fuproc.2018.05.017

[40] J. H. Kwak, J. Hu, D. Mei, C. W. Yi, D. H. Kim; C. H. F. Peden, L. F. Allard, J. Szanyi, Coordinatively unsaturated Al^{3+} centers as binding sites for active catalyst phases of platinum on gamma-Al_2O_3, Science 325 (2009) 1670-1673. DOI: 10.1126/science.1176745

[41] J. H. Kwak, D. Mei, C.-W. Yi, D. H. Kim, C. H. F. Peden, L. F. Allard, J. Szanyi, Understanding the nature of surface nitrates in BaO/γ-Al_2O_3 NOx storage materials: A combined experimental and theoretical study, J. Catal. 261 (2009) 17-22. https://doi.org/10.1016/j.jcat.2008.10.016

[42] R. Bleta, B. Schiavo, N. Corsaro, P. Costa, A. Giaconia, L. Interrante, E. Monflier, G. Pipitone, A. Ponchel, S. Sau, O. Scialdone, S. Tilloy, A. Galia, Robust mesoporous CoMo/γ-Al_2O_3 catalysts from cyclodextrin-based supramolecular assemblies for hydrothermal processing of microalgae: effect of the preparation method, ACS Appl. Mater. Interfaces 10 (2018) 12562-12579. https://doi.org/10.1021/acsami.7b16185

[43] R. Bleta, A. Lannoy, C. Machut, E. Monflier, A. Ponchel, Understanding the role of cyclodextrins in the self-assembly, crystallinity, and porosity of titania nanostructures, Langmuir 30 (2014) 11812-11822. https://doi.org/10.1021/la502911v

[44] S. Koohi Kamali, C. P. Tan, T.C. Ling, Optimization of Sunflower Oil Transesterification Process Using Sodium Methoxide, The Scientific World Journal 2012 (2012). https://doi.org/10.1100/2012/475027

[45] F. R. Abreu, M. B. Alves, C. C. S. Macêdo, L. F. Zara and P. A. Z. Suarez, New multi-phase catalytic systems based on tin compounds active for vegetable oil transesterification reaction, J. Molec. Catal. A: Chemical 227 (2005) 263-267. https://doi.org/10.1016/j.molcata.2004.11.001

[46] G. Sun, F. Qi, Y. Li, N. Wu, J. Cao, S. Zhang, X. Wang, G. Yi, H. Bala and Z. Zhang, Solvothermal synthesis and characterization of ultrathin SnO nanosheets, Material Letters 118 (2014) 69-71. https://doi.org/10.1016/j.matlet.2013.12.048

[47] A. Huda, C. T. Handoko, M. D. Bustan, B. Yudono, F. Gulo, New route in the synthesis of Tin(II) oxide micro-sheets and its thermal transormation, Material Letters 211 (2018) 293-295. https://doi.org/10.1016/j.matlet.2017.10.029

[48] R. Bleta, P. Alphonse, L. Pin, M. Gressier, M. J. Menu, An efficient route to aqueous phase synthesis of nanocrystalline γ-Al$_2$O$_3$ with high porosity: From stable boehmite colloids to large pore mesoporous alumina, J. Colloid Interface Sci. 367 (2012) 120-128. https://doi.org/10.1016/j.jcis.2011.08.087

[49] S. Brunauer, P.H. Emmett, E. Teller, Adsorption of gases in multimolecular layers. J. Am. Chem. Soc. 60 (1938) 309-319. https://doi.org/10.1021/ja01269a023

[50] E. P. Barrett, L. G. Joyner, P. P. Halenda, The determination of pore volume and area distributions in porous substances. I. computations from nitrogen isotherms, J. Am. Chem. Soc. 73 (1951) 373-380. https://doi.org/10.1021/ja01145a126

[51] A. S. Abdel-Naby, R. F. Al-Ghamdi, A. A. Al-Ghamdi, Effect of cyanoguanidine-metal and urea-metal complexes on the thermal degradation of poly(vinyl chloride), J. Vinyl Addit. Techn. 16 (2010) 15-22. https://doi.org/10.1002/vnl.20225

[52] W. Xie, H. Wang, H. Li, Silica-Supported Tin Oxides as Heterogeneous Acid Catalysts for Transesterification of Soybean Oil with Methanol, Ind. Eng. Chem. Res. 51 (2012) 225-231. https://doi.org/10.1021/ie202262t

[53] R. Bleta, C. Machut, B. Léger, E. Monflier, A. Ponchel, Coassembly of block copolymer and randomly methylated β-cyclodextrin: From swollen micelles to mesoporous alumina with tunable pore size, Macromolecules 46 (2013) 5672-5683. https://doi.org/10.1021/ma4008303

[54] R. Bleta, C. Machut, B. Léger, E. Monflier, A. Ponchel, Investigating the effect of randomly methylated β-cyclodextrin/block copolymer molar ratio on the template-directed preparation of mesoporous alumina with tailored porosity, J. Incl. Phenom. Macrocycl. Chem. 80 (2014) 323-335. https://doi.org/10.1007/s10847-014-0405-7

[55] C. Decarpigny, R. Bleta, A. Ponchel, E. Monflier, Oxidation of 2,5-diformfylfuran to 2,5-furandicarboxylic acid catalyzed by *Candida antarctica* Lipase B immobilized in a cyclodextrin-

templated mesoporous silica. The critical role of pore characteristics on the catalytic performance, Colloids Surf. B 200 (2021) 111606. https://doi.org/10.1016/j.colsurfb.2021.111606

[56] Y. Duan, Electronic properties and stabilities of bulk and low-index surfaces of SnO in comparison with SnO_2: A first-principles density functional approach with an empirical correction of van der Waals interactions, Phys. Rev. B *77* (2008) 045332. https://doi.org/10.1103/PhysRevB.77.045332

[57] L.J. Visioli, F. De Castilhos, C. Da Silva, Use of heterogeneous acid catalyst combined with pressurized conditions for esters production from macauba pulp oil and methyl acetate, J Supercrit Fluids 150 (2019) 65-74. https://doi.org/10.1016/j.supflu.2019.03.023

[58] E. Garcica, M. Laca, E. Pecrez, A. Garrido, J. Peinado, New class of acetal derived from glycerin as a biodiesel fuel component, Energy Fuels 22 (2008) 4274-4280. https://doi.org/10.1021/ef800477m

[59] A.L.B. Nunes, F. Castilhos, Chemical interesterification of soybean oil and methyl acetate to FAME using CaO as catalyst, Fuel 267 (2020) 117264. https://doi.org/10.1016/j.fuel.2020.117264

[60] A. K. Endalew, Y. Kiros, R. Zanzi, Inorganic heterogeneous catalysts for biodiesel production from vegetable oils, Biomass Bioenergy 35 (2011) 3787-3809. https://doi.org/10.1016/j.biombioe.2011.06.011

[61] O. Farobie, Y. Matsumura, Continuous production of biodiesel under supercritical methyl acetate conditions: experimental investigation and kinetic model, Bioresour Technol 241 (2017) 720-725. https://doi.org/10.1016/j.biortech.2017.05.210

[62] D. D. MacDonald, P. Butler, The thermodynamics of the aluminium-water system at elevated temperatures, Corros. Sci. 13 (1973) 259-274. https://doi.org/10.1016/0010-938X(73)90004-8

[63] R. M. Ravenelle, J. R. Copeland, W. G. Kim, J. C. Crittenden, C. Sievers, Structural changes of γ-Al_2O_3-supported catalysts in hot liquid water, ACS Catal. 1 (2011) 552-561. https://doi.org/10.1021/cs1001515